https://doi.org/10.15360/1813-9779-2026-1-2618

Argon-Oxygen Mixture as a Multisystem Therapy after Circulatory Arrest: an Experimental Study

Ekaterina A. Boeva*, Sergey N. Kalabushev, Lidia A. Varnakova, Maxim A. Lyubomudrov, Zoya I. Tsokolaeva, Artem N. Kuzovlev, Victor V. Moroz, Ivan F. Ostreykov, Elena A. Spiridonova, Ivan A. Ryzhkov

V. A. Negovsky Research Institute of General Reanimatology, Federal Research and Clinical Center of Intensive Care Medicine and Rehabilitology, Ministry of Education and Science of Russia, 25 Petrovka Str., Bldg. 2, 107031 Moscow, Russia

For citation: *Ekaterina A. Boeva, Sergey N. Kalabushev, Lidia A. Varnakova, Maxim A. Lyubomudrov, Zoya I. Tsokolaeva, Artem N. Kuzovlev, Victor V. Moroz, Ivan F. Ostreykov, Elena A. Spiridonova, Ivan A. Ryzhkov.* Argon-Oxygen Mixture as a Multisystem Therapy after Circulatory Arrest: an Experimental Study. *Obshchaya Reanimatologiya = General Reanimatology.* 2026; 22 (1): 26–40. https://doi.org/10.15360/1813-9779-2026-1-2618 [In Russ. and Engl.]

***Correspondence to:** Ekaterina A. Boeva, eboeva@fnkcrr.ru

Summary

Cardiac arrest remains one of the leading causes of death worldwide. Even with successful resuscitation, patient outcomes are often poor due to post-resuscitation syndrome, which includes cerebral hypoxia, myocardial dysfunction, microcirculatory disorders, coagulation abnormalities, and systemic inflammation. Argon, an inert noble gas, has neuroprotective and cardioprotective properties, making it a promising candidate for early post-resuscitation therapy.

The aim of the study was to evaluate the organoprotective properties of an argon-oxygen mixture when inhaled in the early post-resuscitation period for 2 hours after asphyxial circulatory arrest in rats.

Materials and methods. A prospective randomized controlled experimental study was conducted on male Wistar rats ($n=43$) using an asphyxial circulatory arrest model. The animals were divided into three groups: sham-operated (SO, $n=12$), circulatory arrest with resuscitation (CA, $n=13$), and circulatory arrest with resuscitation and two-hour inhalation of a 70%/30% argon-oxygen mixture in the post-resuscitation period (CA+iAr, $n=18$). Hemodynamics, microcirculation, blood gas composition, coagulation (low-frequency piezothromboelastography), neurological status, and biomarkers of organ damage were evaluated. Beclin-1 and caspase-3 expression was analyzed immunohistochemically.

Results. Argon inhalation did not have a significant effect on systemic hemodynamics, but it was accompanied by improved tissue oxygenation and metabolism: a decrease in blood lactate ($p=0.043$), an increase in the p/F oxygenation index ($p=0.001$), and stabilization of microcirculation variability (Kv, σ). Statistically significantly increased expression of the Beclin-1 protein in the lungs, myocardium, and hippocampus reflected activation of autophagy. In the CA+iAr group, there was an improvement in neurological status compared to CA ($p=0.02$), a decrease in serum neuron-specific enolase ($p=0.011$), and a decrease in the number of caspase-3-positive cells ($p=0.011$), indicating a reduction in apoptosis and damage to the nervous tissue. Argon had a moderate anticoagulant and antiplatelet effect (coagulation drive intensity — CDI, and maximum clot firmness-MCF reduction), while maintaining normal processes of clot retraction and lysis. The electrophysiological parameters of the heart (QRS, QTc) varied within the physiological range, indicating the absence of pro-arrhythmic effects in argon.

Conclusion. Early inhalation of argon-oxygen mixture after circulatory arrest has a multisystem protective effect: improves oxygenation and microcirculation, promotes activation of autophagy mechanisms in vital organs, reduces the severity of neuronal damage, and modulates blood clotting in some measure. Argon can be considered a promising therapeutic agent for post-resuscitation syndrome. Further clarification is needed to assess argon's molecular mechanisms of action and long-term outcomes after its use.

Keywords: argon-oxygen mixture; circulatory arrest; post-resuscitation syndrome; neuroprotection; cardioprotection; autophagy; Beclin-1; microcirculation; coagulation; apoptosis; neuron-specific enolase

Conflict of interest. The authors declare no conflict of interest.

Information about the authors/Информация об авторах:

Ekaterina A. Boeva/Екатерина Александровна Боева: https://orcid.org/0000-0002-0422-5018
Sergey N. Kalabushev/Сергей Николаевич Калабушев: https://orcid.org/0000-0001-7017-7897
Lidia A. Varnakova/Лидия Александровна Варнакова: https://orcid.org/ 0000-0003-4420-1923
Maxim A. Lyubomudrov/Максим Алексеевич Любомудров: https://orcid.org/0000-0002-1735-592X
Zoya I. Tsokolaeva/Зоя Ивановна Цоколаева: https://orcid.org/0000-0003-2441-6062
Artem N. Kuzovlev/Артем Николаевич Кузовлев: https://orcid.org/0000-0002-5930-0118
Victor V. Moroz/Виктор Васильевич Мороз: https://orcid.org/0000-0002-5930-5457
Ivan F. Ostreykov/Иван Федорович Острейков: https://orcid.org/0000-0002-4863-1958
Elena A. Spiridonova/Елена Александровна Спиридонова: https://orcid.org/0000-0002-5230-5725
Ivan A. Ryzhkov/Иван Александрович Рыжков: https://orcid.org/0000-0002-0631-5666

Read the full-text English version at www.reanimatology.com

Introduction

Cardiovascular arrest remains one of the leading causes of death worldwide, despite significant advances in cardiopulmonary resuscitation (CPR) and intensive care [1–3]. Even with successful resuscitation and return of spontaneous circulation (ROSC), the prognosis for such patients often remains extremely poor due to severe post-resuscitation syndrome (PRS). Post-cardiac arrest syndrome (PCAS) is a multiorgan pathology that includes cerebral hypoxia, myocardial dysfunction, systemic inflammation, and reperfusion injury. All these components together contribute to high mortality in the first 24 hours and the development of adverse neurological outcomes in survivors. In view of this, the search for effective multisystem therapeutic strategies capable of influencing the main constituents in post-resuscitation damage becomes particularly relevant [4–9].

In recent years, there has been growing interest in the use of inert gases, particularly xenon and argon, as potential organoprotectors. Xenon, which has demonstrated a noticeable neuroprotective effect in a number of preclinical and clinical studies, is limited in its use due to its high cost and handling difficulties [10–13]. Unlike xenon, argon is readily available, more stable, and has a favorable safety profile. In addition, argon exhibits a wide range of biological effects, including anti-apoptotic, antioxidant, and anti-inflammatory, making it a promising candidate for comprehensive treatment of systemic ischemic damage [14–20].

Experimental studies on various models of ischemic and traumatic damage to the central nervous system have demonstrated that inhalation of argon reduces the volume of cerebral damage, reduces the activation of microglia and astrocytes, and modulates the expression of pro-inflammatory cytokines [17, 18, 20]. However, the effects of argon on other organs and systems, especially in the context of global ischemia, such as circulatory arrest, remain poorly understood. There are some publications indicating presumable cardioprotection and stabilization of hemodynamics when argon is used, but there is a lack of systematic data on its multisystem effects after circulatory arrest [21–26].

The model of asphyxial circulatory arrest in rats provides a reliable and reproducible platform for assessing both neurological and somatic sequelae of post-resuscitation injury. It allows for the study of the subtle mechanisms of reperfusion syndrome, coagulation disorders, systemic inflammation, and respiratory failure under controlled experimental conditions [27]. The use of this model to evaluate the action of argon provides an opportunity for an objective assessment of its organoprotective effects in conditions closest to clinical resuscitation practice.

It is important to emphasize that modern resuscitation medicine requires not only protocols for successful CPR, but also therapeutic interventions capable of improving the survival and quality of life of surviving patients. Given the high mortality rate within the first 24 hours after ROSC, early intervention in the post-resuscitation period is of particular importance. In this regard, argon, which has high bioavailability and can be rapidly administered by inhalation, appears to be a very convenient and promising agent for use immediately after return of spontaneous circulation.

Thus, based on existing data on the potential organoprotective effects of argon, as well as the limited availability of clinically applicable multisystem therapies in the early post-resuscitation period, there is a need for more in-depth research into this approach. The availability of preclinical data on the neuroprotective and cardioprotective effects of argon requires verification in the context of complex post-resuscitation syndrome, which includes damage to the lungs, heart, and hemostasis systems.

Objective: to evaluate the organoprotective properties of inhaled argon-oxygen mixture in the early post-resuscitation period within 2 hours after asphyxial cardiac arrest in rats.

Materials and Methods

Study characteristics. A prospective randomized controlled experimental study was conducted on laboratory animals in vivo. The study was conducted in accordance with accepted national and international bioethical standards [28]. The study protocol was approved by the local Ethics Committee of the Federal Scientific and Clinical Center for Intensive Care Medicine and Rehabilitology of the Ministry of Education and Science of Russia (1/23/4, 05.04.2023).

Study subject. Male Wistar rats, $n=43$. Weight: 200–250 g. The animals were kept in standard vivarium conditions, in social groups, with unlimited access to filtered tap water and complete feed, under artificial lighting in a 12/12 hour day/night cycle.

Group I ($n=12$) — Sham-operated animals (SO);

Group II ($n=13$) — Asphyxial cardiac arrest with resuscitation (CA).

Group III ($n=18$) — Asphyxial cardiac arrest with resuscitation and argon inhalation in the post-resuscitation period (CA+iAr).

Experimental procedures

Anesthesia. Animals were given combined anesthesia: tiletamine/zolazepam (Zoletil 100, Virbac, France) 20 mg/kg + xylazine («Xylanit», NITA-PHARM LLC, Russia) 5 mg/kg intraperitoneally. If the depth of anesthesia decreased (response to pain stimulus), an additional injection of Zoletil 100 10 mg/kg intraperitoneally was administered.

Catheterization of major vessels. For invasive measurement of blood pressure (BP) and arterial blood sam-

pling, the left carotid artery was catheterized with a PE-50 polyethylene catheter (OD 0.95 mm, ID 0.58 mm, SciCat, Russia). For the purpose of intravenous administration of pharmaceuticals during resuscitation measures, infusion therapy, and maintenance therapy in the post-resuscitation period, the right jugular vein was catheterized. Catheter heparinization regimen: administration of 0.2 ml of unfractionated heparin solution (5 IU/ml) after placement and subsequently 0.1–0.2 ml as needed.

Tracheal cannulation. The anesthetized animal was fixed in a supine position on a surgical platform. Tracheal cannulation was performed by a surgeon under visual control of the trachea through an incision in the skin and soft tissues on the anterior surface of the neck (during vascular catheterization). Under visual control, tracheal cannulation was performed with a 16G venous catheter. The tube was fixed to the animal's cheek with a surgical suture. The animal was connected to a ventilator. Rocuronium bromide was administered intravenously at a dose of 1.4 mg/kg body weight.

Preparatory measures. After tracheal cannulation and administration of a muscle relaxant, mechanical ventilation of the lungs was initiated in CMV/VC mode (FiO_2 0.21, f 60/min, I:E 1:2, Vt according to the nomogram for rats). The rat was fixed in a supine position on a heated platform of the MouseMonitor S monitor (INDUS Instruments, USA). Central body temperature was measured and monitored using a rectal thermometer. Target temperature values: 36.0–37.0°C. To prevent heat loss, the animal was covered with insulating material. The stabilization period before the start of measurements was 15 minutes.

Blood pressure measurement. An arterial catheter was connected to a Deltran DPT-100 transducer (Utah Medical Products, USA) using a tee-joint and infusion line. The analog pressure signal from the transducer and the BP-100 device was transmitted to a PowerLab16/35 device (ADInstruments, Australia) connected to a PC. The digitized BP signal was stored in the PC hard drive memory and analyzed using LabChart Pro 8 software (ADInstruments, Australia). Based on the BP curve, the mean arterial pressure (MAP) was calculated for the measurement period (5 minutes).

Electrocardiogram (ECG) recording. The analog ECG signal from the surface electrodes of the MouseMonitor S platform (INDUS Instruments, USA) was transmitted to the PowerLab16/35 device (ADInstruments, Australia) connected to a PC. The digitized ECG signal in three standard leads (I, II, III) was stored in the PC hard drive memory and analyzed using LabChart Pro 8 software. Based on the ECG data, the average heart rate (HR) was calculated for the measurement period (5 minutes).

Registration of local skin blood flow. Microcirculation in rat skin was assessed non-invasively using laser Doppler flowmetry (LDF). The rat's tail was wiped with a damp gauze pad to clean the skin surface. The optical probe of the LAZMA MC-3 device (LLC NPP «LAZMA», Russia) was placed perpendicularly at the border between the middle and proximal thirds of the animal's tail (on the ventral side). The duration of LDF registration was 5 minutes. The following parameters were analyzed: average perfusion value (M, p. u.); mean square deviation of blood flow amplitude (σ, p. u.) – a measure of individual temporal variability of perfusion; perfusion variation coefficient (Kv=σ / M, %). Based on the measurements, cutaneous vascular conductance (CVC=M / MAP, p. u. / mm Hg) was also calculated.

Measurement of gas composition and acid-base balance (ABB) of arterial blood. An arterial blood sample (0.2 ml) was taken from an arterial catheter into a heparinized insulin syringe (1.0 ml). Analysis of arterial blood gases and ABB (pH, pCO_2, pO_2, BE, HCO_3^-, SaO_2, lactate) was performed using CG4+ reagent cartridges for the iSTAT 1 analyzer (Abbott Point of Care Inc., USA).

Experimental model of circulatory arrest and resuscitation measures. We used a previously described experimental model of asphyxial circulatory arrest in rats [27], to which we made a number of modifications in accordance with the objectives of this study. After recording the baseline parameters, the animal was re-administered a muscle relaxant (rocuronium bromide 1.4 mg/kg), after which mechanical ventilation was discontinued. ECG and blood pressure monitoring was continued to determine the moment of circulatory arrest. When the mean arterial pressure fell below 20 mm Hg along with extreme bradycardia (or other pathological rhythm), effective tissue perfusion was considered absent, and the time of circulatory arrest was counted. After 2 minutes (no-flow time), resuscitation measures were initiated. Mechanical ventilation was resumed in CMV/VC mode with the following parameters: FiO_2 1.0, f 80/min, I:E=1:2, Vt according to the nomogram for rats. Chest compressions were performed in the anterior-posterior direction with the rat lying on its back at a frequency of 200 per minute. Intravenous adrenaline was administered at a dose of 0.005 mg/kg. After a one-minute cycle, chest compressions were stopped, and heart rate and blood pressure were assessed. If necessary, adrenaline was re-administered at a dose of 0.005 mg/kg. At the same time, ECG, blood pressure, and LDF monitoring continued.

After return of spontaneous circulation (ROSC), we continued mechanical ventilation with 100% O_2, monitoring blood pressure and ECG, and also infusion of 0.9% NaCl solution at a rate of 10 ml/kg/h. Five minutes after resuscitation, the gas composition and CO_2 content of arterial blood were assessed, and the parameters of mechanical ventilation were adjusted accordingly. In cases of severe metabolic acidosis (pH < 7.1, BE < –10 mmol/L), a 5% NaHCO3 solution was infused at a dose of 1 mmol/kg. Next, depending on the group, a mixture of argon and oxygen (70%/30%) or 30% oxygen and air (in the SO and CA groups) was supplied to the ventilator circuit for 2 hours. In the SO group, the same procedures and measurements were performed as in the CA group, except for cardiac arrest and resuscitation (without administration of adrenaline and bicarbonate, but with infusion, anesthesia, and muscle relaxants according to the study plan). Two hours after the resuscitation period (after completing

the measurements), a test for spontaneous breathing was performed: the breathing circuit was disconnected from the endotracheal tube, and the frequency, depth, and pattern of breathing were assessed. Observation of the animal and warming continued for another hour. At the end of this period, the general condition and neurological status were assessed. The general scheme of the experiment is presented in Fig. 1.

Assessment of neurological status. Neurological deficit was assessed using the General Neurological Score (GNS) scale. Motor and sensory tests (vibrissae, vision), reflexes (corneal, pain, ear), balance, and coordination were assessed. The maximum score was 1, the minimum score was 0. The maximum total score was 10.

Euthanasia. The animal was euthanized by intravenous administration of 2 ml of 4% KCl solution under general anesthesia with zoletil (additional dose of 20 mg/kg i/v).

Examination of the hemostasis system using low-frequency piezoelastography. The examination was performed using a Mednord NPTEG thromboelastograph (Mednord–Technika, Russia), with a blood sample volume of 0.5 ml. NPTEG parameters were measured immediately after blood collection. No more than 10 seconds elapsed between blood collection and sample placement in the analyzer. The collected blood was transferred from the syringe to a special test tube for analysis. After placing the test tube in the device, the analyzer needle was inserted into the blood and the curve was recorded by pressing the Start button in the software window that came with the device. The curve recording lasted from 30 to 40 minutes, which allowed most of the recorded indicators to be captured for analysis:

Ai — amplitude (clot density) at a specific time point from 0 to 6, expressed in conventional units.

ti — time of completion of a specific coagulation phase (min.).

ICC — intensity of the contact phase of coagulation; quotient of the difference in amplitudes (A0—A1) for the reaction period t1.

TAC — thrombin activity constant; quotient of the amplitude A2 = (100 const) divided by time (t2—t1).

CDI — coagulation drive intensity; quotient of the difference in amplitudes (A3—A1) divided by blood clotting time t3.

CPI — clot polymerization intensity; quotient of the difference in amplitudes (A4—A3) divided by a constant time = 10 min.

MCD — maximum clot density; the difference between the values (A5—A1) in relative units, characterizes the maximum clot density due to platelet activity and the quantitative/qualitative characteristics of cross-linked fibrin.

CRLI — clot retraction and lysis intensity; determined as the percentage by which the clot amplitude decreases within 10 minutes after reaching MCD: (A5—A6) / A5 × 100%

TAAC — total anticoagulant activity coefficient; quotient of the division of CDI/CPI.

After completing the measurement, the cuvette with blood was disposed of, and the analyzer needle was carefully cleaned with a cotton swab moistened with saline solution. The next measurement was started no earlier than 5 minutes after cleaning the needle.

Study of serum concentrations of biomarkers of brain damage. Serum concentrations of brain injury biomarkers (neuron-specific enolase, NSE) were measured using enzyme-linked immunosorbent assay (ELISA) in accordance with the manufacturer's instructions for ELISA kits (Cloud-Clone Corp., USA). Recording time: once at the end of the experiment.

Immunohistochemical analysis. Fixation was performed in 10% buffered formalin (Biovitrum, Russia) for 48 hours (the volume of the fixing fluid was at least 15 times greater than the volume of the material). Standard processing of the material included washing in tap water, dehydration in alcohols of increasing concentration, and embedding in low-melting paraffin. Sections 2–3 μm thick were prepared on a rotary microtome. The sections were stained with hematoxylin and eosin. Morphometric examination of brain areas highly sensitive to hypoxia (sensory-motor cortex, CA1 and CA4 fields of the hip-

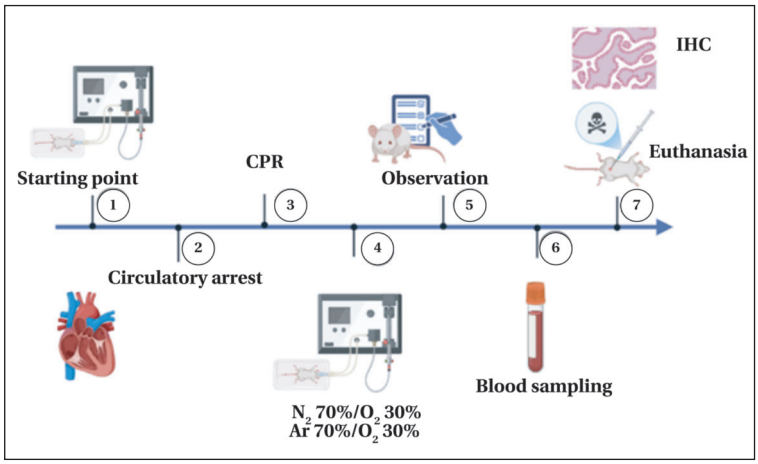

Fig. 1. General experimental setup.
Note.
1. Initial condition (after anesthesia, catheterization, and stabilization). Recording of parameters at the first time point: ECG, blood pressure, local skin blood flow, blood gas analysis, thromboelastography (TEG).
2. Simulation of circulatory arrest.
3. Cardiopulmonary resuscitation.
4. 10 minutes after resuscitation and return of spontaneous circulation. Recording of parameters at the second time point: ECG, blood pressure, local skin blood flow, blood gas analysis. Supply of argon-oxygen or oxygen-air mixture depending on the group being studied.
5. 120 minutes after the resuscitation period, weaning from ventilator and transition to spontaneous breathing after measurements. Recording of parameters at the third time point: ECG, blood pressure, local skin blood flow, blood gas analysis, TEG; assessment of neurological status.
6. Blood tests measuring ABB, thromboelastography parameters, and neuron-specific enolase content.
7. Euthanasia. IHC.

pocampus) was performed using microphotographs taken with a microscope slide scanner (Aperio ScanScope CS, Aperio, Vista, CA, US), a Nikon Eclips Ni-U microscope, and NIS-Elements BR software (Nikon Corp., Japan).

For immunohistochemical analysis, sections were prepared: deparaffinization and antigen retrieval of paraffin sections were performed using Trilogy® Pretreatment Solution Cell Marque, according to the manufacturer's protocol. The sections were then washed twice in PBS for 5 minutes and endogenous peroxidase was blocked with 2% hydrogen peroxide for 10 minutes. The sections were then washed twice in PBS for 5 minutes. To prevent nonspecific binding of primary or secondary antibodies to tissue proteins, Protein Block Serum-free ab64226 Abcam (Cambridge, UK) was used with 30 minutes of exposure in a humid chamber. The sections were then washed twice in PBS for 5 minutes. Antibodies to Caspase-3 (Invitrogen. PA5-77887 1:200) and beclin (Ab62557 1:200) diluted in Antibody and Diluent (ab64211 abcam) were incubated in a humid chamber at 37°C for 1 hour. The sections were then washed twice in PBS for 5 minutes. For visualization, secondary antibodies with peroxidase UMR1000PD-BMS (Diagnostic Biosystems, USA) were used according to the manufacturers' protocol. The sections were then washed twice in PBS for 5 minutes, developed with DAB, stained with hematoxylin for 1–2 minutes, dehydrated with 70%, 96%, and 100% alcohol, and xylene was added in two stages.

The data were statistically processed using SPSS Statistics (IBM SPSS Statistics for Windows, version 27.0.1, Armonk, NY, USA) and GraphPad Prism (version 8.0.1, Boston, MA, USA). The normality of distribution was checked using the Shapiro–Wilk test. The data were presented as the mean and standard deviation, as well as *Me* (*Q1*; *Q3*), where Me is the median, *Q1* is the first quartile (25th percentile), and *Q3* is the third quartile (75th percentile), depending on the type of distribution. For the analysis of quantitative data, the Kruskal–Wallis test with post-hoc analysis (Benjamin–Krieger–Yekutieli adaptive method) and the Mann–Whitney test (Wilcoxon rank sum) were used. To compare categorical variables, we used the χ^2 test or Fisher's exact test (for event frequencies less than 10%). Correlation analysis was performed using Spearman's method, and two-tailed tests were used in all analyses. Values of $p<0.05$ were considered statistically significant.

Results

At the first time point (before induction of asphyxia), two fatalities were registered in the CA group due to complications of anesthesia. Necropsy of the animals revealed no pathological changes in the internal organs. The remaining animals underwent modeling without reaching the criteria for humane euthanasia at any stage of the experiment. The average body weight of rats in the CA+iAr, CA, and SO groups at the time of inclusion in the experiment was 249.3±18.3, 245.6±18.9, and SO 248.1±15.4 g., respectively, and did not differ between groups ($p>0.05$).

Hemodynamic parameters. Fig. 2 shows the blood pressure (BP) and heart rate (HR) parameters in the study groups. At baseline (1), BP and HR values were within the physiological norm and did not show statistically significant intergroup differences (BP: SO 77.0 (73.8; 82.3) vs CA 78.0 (69.3; 88.9), $p=0.825$; SO vs CA+iAr 76.4 (69.3; 83.0), $p=0.752$; CA vs CA+iAr, $p=0.946$. HR: SO 241.6 (209.4; 250.9) vs CA 251.7 (240.0; 259.8), $p=0.545$; SO vs CA+iAr 250.1 (240.5; 261.1), $p=0.281$; CA vs CA+iAr, $p=0.812$).

At the second time point after return of spontaneous circulation, a statistically significant increase in blood pressure and a compensatory increase in heart rate were observed both within the CA and CA+iAr groups and in comparison with the SO group (BP: SO 74.1 (67.2; 92.9) vs CA 125.6 (79.5; 146.3), $p=0.017$; SO vs CA+iAr 122.5 (106.1; 138.9), $p=0.005$. HR: SO 248.1 (226.0; 256.4) vs CA 345.2 (332.8; 368.9), $p<0.0001$; SO vs CA+iAr 334.2 (291.5; 402.9), $p<0.0001$). No differences between the CA and CA+iAr groups were found for these parameters (BP: $p=0.959$; HR: $p=0.927$).

At the third time point, normalization of BP parameters was recorded (SO 79.05 (72.9; 93.9) vs CA 70.6 (64.5; 76.6), $p=0.065$; SO vs. CA+iAr 69.1 (64.5; 73.2), $p=0.231$, CA vs. CA+iAr, $p=0.873$) and of HR, no significant intergroup differences were found (Fig. 2).

Microcirculation and blood flow variability. No significant intergroup differences in the mean microcirculation (perfusion) index M were observed at any time point. It was found that the CVC index differed statistically significantly between the SO group and the CA group at the second time point ($p=0.042$), as well as in the CA group between the first and second points ($p<0.0001$), the 2nd and 3rd points ($p=0.04$), and in the CA+iAr group between the 1st and 2nd time points ($p=0.01$). σ and Kv showed a clear dependence on the experimental conditions. In the SO group, the values of σ and Kv remained relatively stable and were within the physiological norm.

At the 3rd time point, a statistically significant decrease in the values of σ and Kv was noted in the CA+iAr group compared to the CA group ($p=0.002$; $p=0.007$, respectively), as well as with the SO group ($p=0.007$; $p=0.016$, respectively) (Fig. 3).

Acid-base balance (ABB) and tissue metabolism indicators. After return of spontaneous circulation (point 2), statistically significant differences in lactate, BE, p/F, and pH were observed in the CA and CA+iAr groups compared to the SO group (Fig. 4). The condition of the animals at this time point was characterized by mixed metabolic acidosis and impaired tissue perfusion. 120 minutes after resuscitation (point 3), gas exchange and ABB parameters were compensated in all groups of animals.

The content of beclin-1 positive cells in the lung tissue was statistically significantly higher in

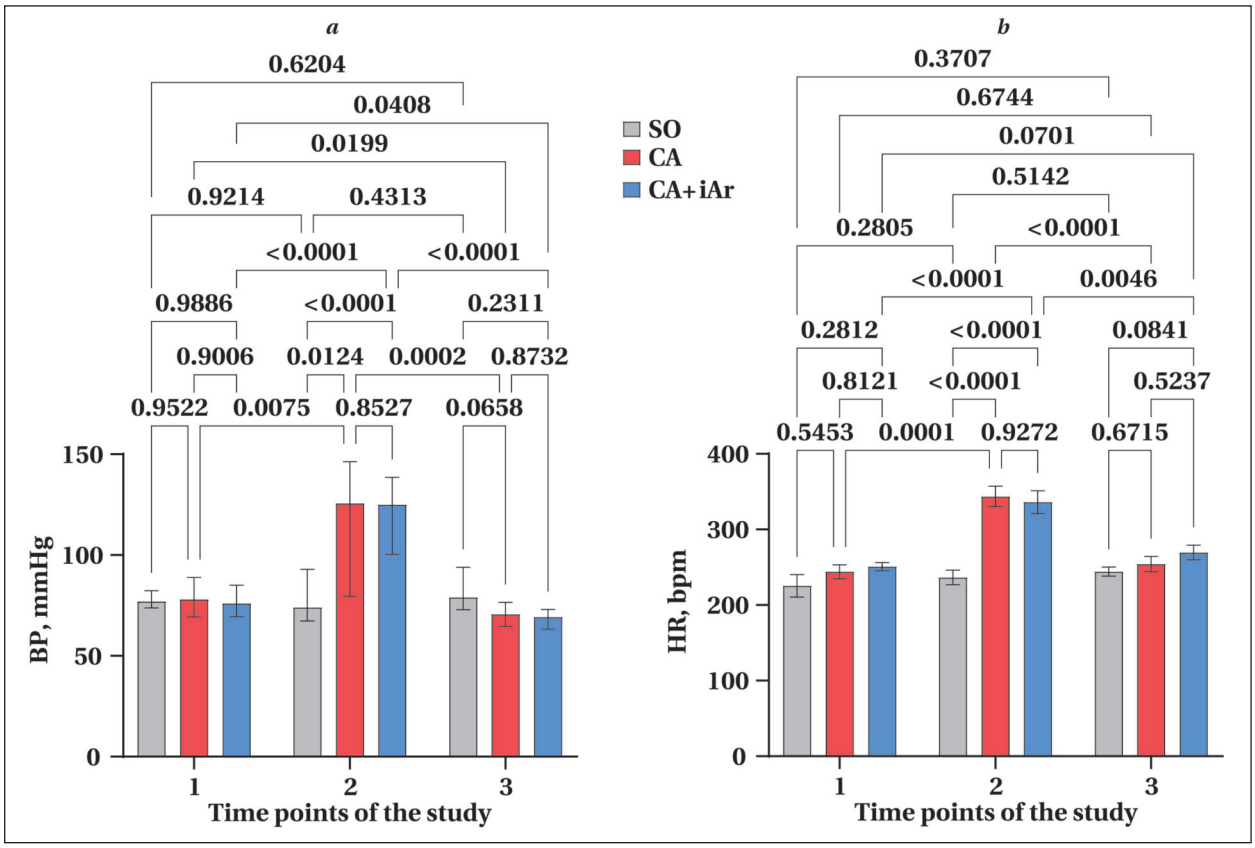

Fig. 2. Blood pressure (*a*) and heart rate (*b*) parameters in the study groups.
Note. In Figs. 2–9, the data are presented as medians and quartiles with indicated *p*-values.

the CA+iAr group (2343 (1558.5; 6528.2) compared to the CA group (1000 (856; 1251.7)), $p=0.028$

Coagulation parameters. The integral parameters of blood coagulation system, reflecting the dynamics of clot formation and subsequent transformation, were analyzed. In the CA+iAr group, we observed a decrease in contact activation intensity (CAI) and a decrease in maximum clot density (MCD), as well as lower polymerization intensity (PI) and coagulation drive (CD) indices (Fig. 6).

Electrophysiological parameters (ECG). The QTc time was longer in the CA+iAr group compared to the SO group (0.120 [0.112; 0.131] s vs. 0.1059 [0.1023; 0.116] s, $p=0.012$), and a difference in QRS duration was found between CA and CA+iAr ($p=0.016$). However, the changes in the intervals were within the reference limits. ST segment changes between groups did not differ statistically (SO 0.17 (0.09; 0.21) vs CA 0.17 (0.15; 0.24), $p=0.321$; SO vs CA+iAr 0.14 (0.11; 0.19), $p=0.423$; CA vs CA+iAr, $p=0.233$) (Fig. 7).

In the CA+iAr group, the content of beclin-1 cells in the myocardium was statistically significantly higher compared to the CA group (2050 (1883; 3582) vs 610.5 (289; 1867.2), $p=0.038$).

Neurological status parameters and markers of organ damage. The total score for the neurological status of animals in the CA group (2 [1.5; 3.5]) was statistically significantly lower than in the CA+iAr group (4.5 [4.0; 5.5]; $p=0.021$) and the SO group (8.5 [6.3; 9.0]; $p=0.0001$) (Fig. 8, *a*).

The beclin-1 protein content in the brain was statistically significantly higher in the CA+iAr group compared to the SO group (3902 (3544; 5212 vs 1080 (379; 1759; $p=0.0003$).

The number of caspase-3+ positive cells was statistically significantly lower in the CA+iAr group compared to the CA group ($p=0.011$). In addition, the content of neuron-specific enolase was statistically significantly lower in animals of the CA+iAr group (16.27 (11.12; 40.7) ng/ml) than in animals in the CA group (29.87 (20.38; 112.19) ng/ml), $p=0.011$ (Fig. 9, *b*).

Discussion

The data obtained indicated the preservation of the basic mechanisms of cardiovascular system regulation under the studied conditions of argon-oxygen mixture inhalation in a model of asphyxial cardiac arrest in rats.

The absence of statistically significant changes in blood pressure and heart rate between the groups allowed us to conclude that the interventions had no effect on macro-hemodynamics, and that identified trends were compensatory in nature.

At the third time point, lactate was statistically significantly lower ($p=0.043$) and the p/F ratio (PaO_2/FiO_2, oxygenation index) was higher ($p=0.001$)

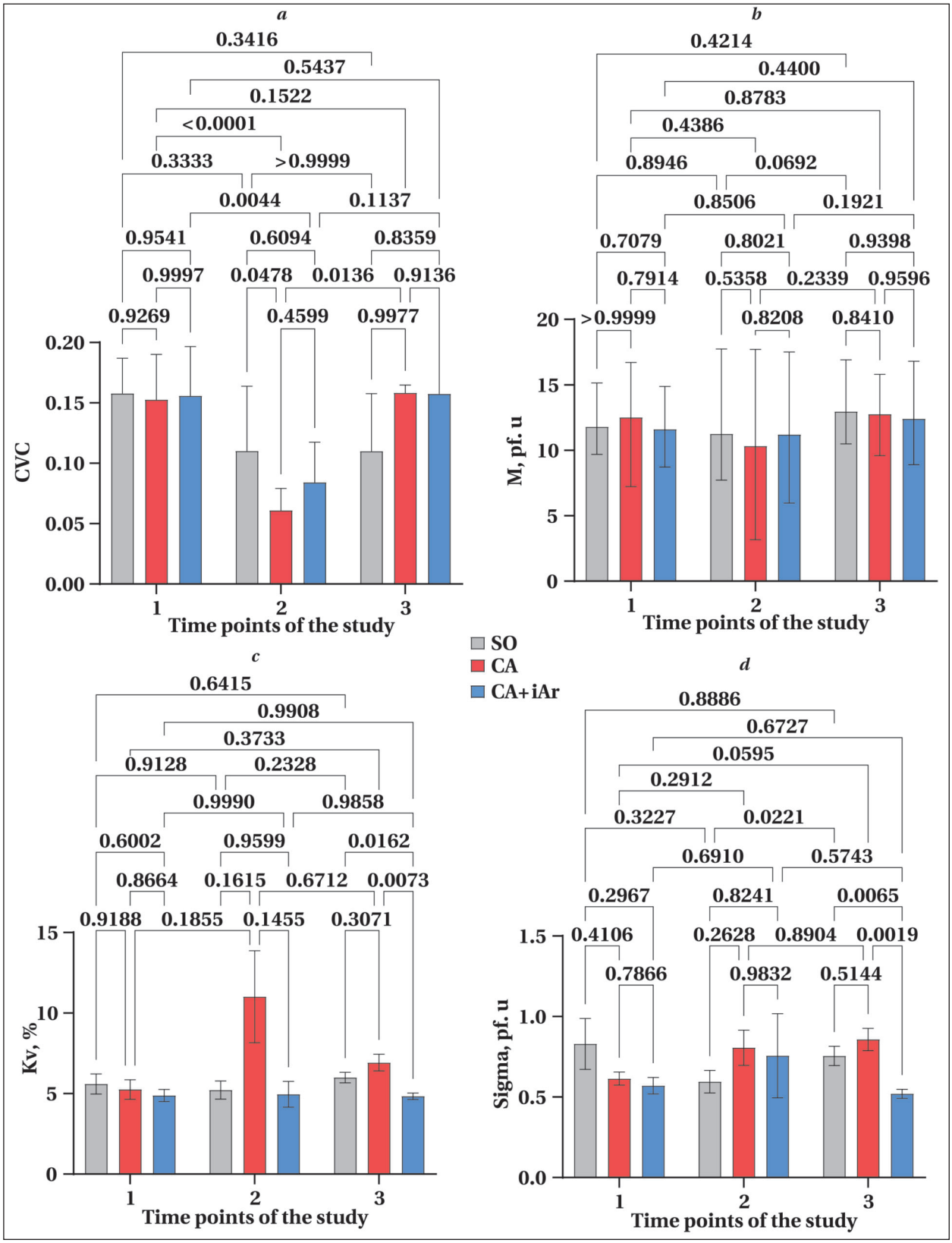

Fig. 3. Microcirculation parameters CVC (*a*), M (*b*), Kv (*c*), Sigma (*d*) in the study groups.

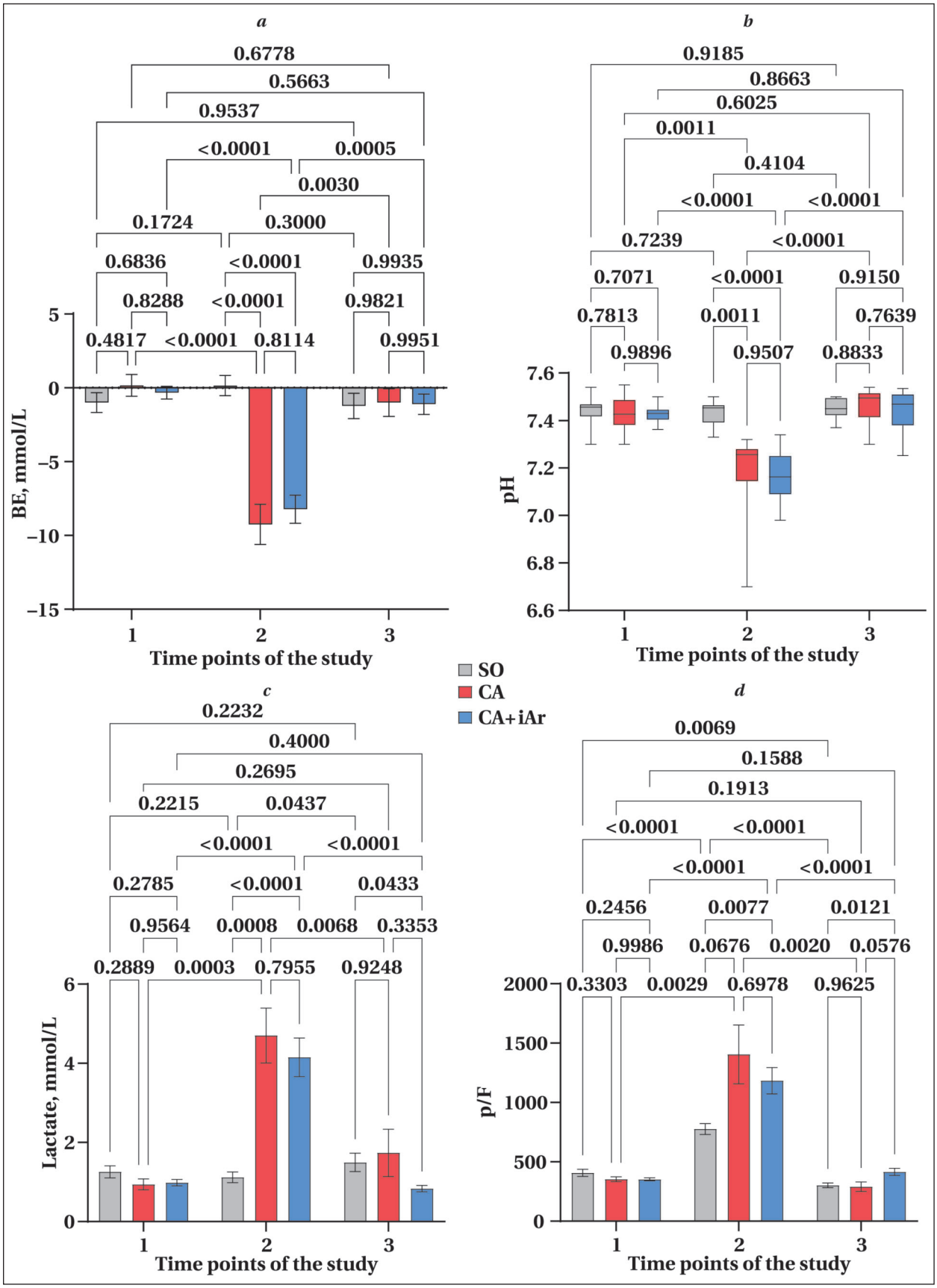

Fig. 4. Indicators of acid-base balance (ABB) and tissue metabolism in the study groups.

in the CA+iAr group than in the SO group (Fig. 4). But there was no significant difference in lactate and p/F between the CA and SO groups. The decrease in lactate combined with an increase in the p/F ratio indicated an improvement in tissue oxygenation and microcirculation following argon therapy.

The decrease in Kv and σ values combined with lower lactate level and increased p/F ratio in the CA+iAr group suggests that argon has a stabilizing effect on microcirculation, optimizing uniform tissue capillary perfusion and reducing blood flow amplitude fluctuations. This is accompanied by optimization of gas exchange and improved tissue oxygenation, by a decrease in anaerobic metabolism, which is confirmed by a decrease in lactate level. At the same time, systemic hemodynamic parameters (BP and HR) remained unchanged, indicating a local, microcirculatory effect of argon that does not affect overall blood flow.

An increase in the amount of beclin-1 in lung tissue in the AC+iAr group may indicate more intense activation of autophagic processes in response to ischemic-reperfusion injury.

The intensification of this process in lung tissue can be interpreted as a manifestation of a protective effect aimed at limiting structural and functional damage. Comprehensive assessment of the respiratory functional parameters confirm this assumption. Increased counts of these cells in the lung tissue after inhalation of argon-containing gas mixture can be considered a marker of protective cellular mechanisms activation aimed at preserving the structural integrity and functional activity of the tissue. In combination with improved gas exchange and oxygen consumption, this indicates a systemic protective effect of argon, actualized through molecular mechanisms of autophagy and through optimization of respiratory and metabolic function.

Thromboelastogram analysis identified changes in coagulation parameters indicating slower clot formation and reduced clot firmness in the presence of argon. At the same time, the thrombin activity constant (TAC) in the CA+iAr group was higher, which indicated a more «compact» and rapid development of the early enzymatic stage of thrombin formation necessary to initiate the coagulation cascade (Fig. 6).

It is important to emphasize that the indicators reflecting clot retraction and subsequent lysis (CRLI), as well as the balance between the rate of amplitude increase and polymerization (TAAC — total anticoagulant activity coefficient), did not show statistically significant changes. This means that argon did not enhance clot lysis processes, and its effect was largely related to how the clot is formed — to the quality of platelet interaction and the structure of polymerizing fibrin.

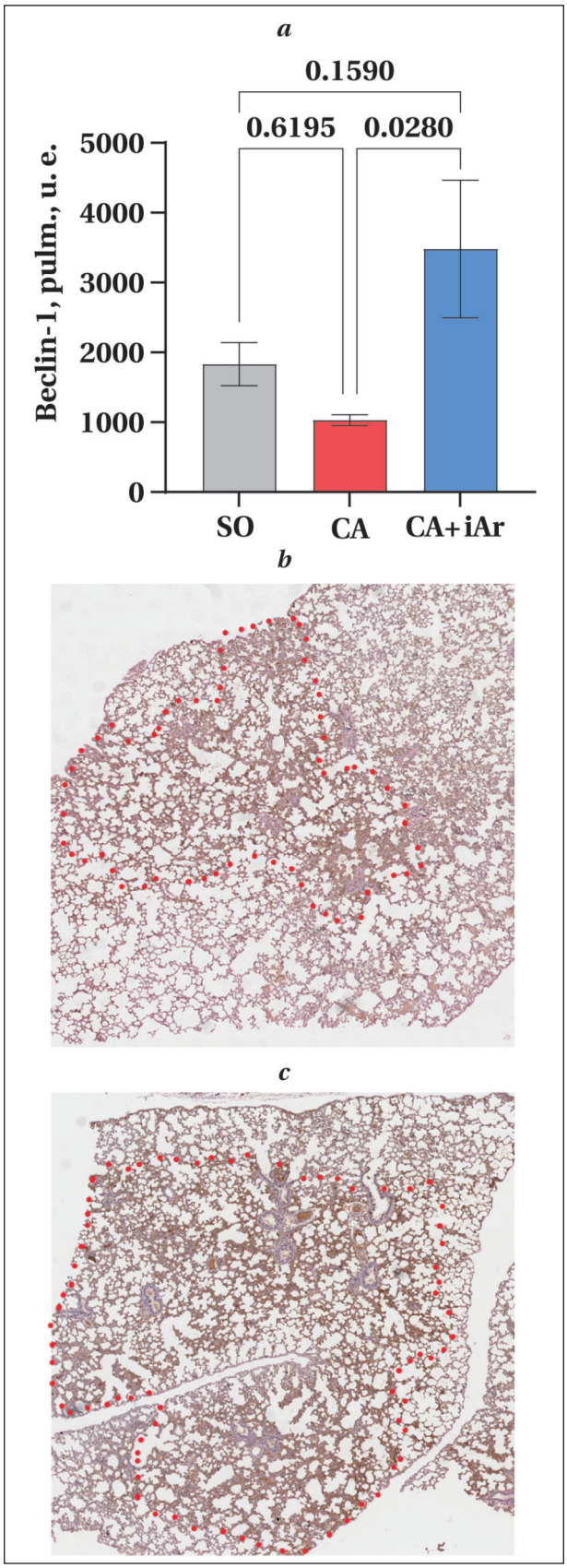

Fig. 5. Number of beclin-1-positive cells in the lungs (*a*). Images representing lung tissue slides in the CA (*b*) and CA+iAr (*c*) groups.
Note. Beclin-1 was evaluated by immunohistochemistry after euthanasia. The red dotted line marks the area that is positively stained for beclin-1.

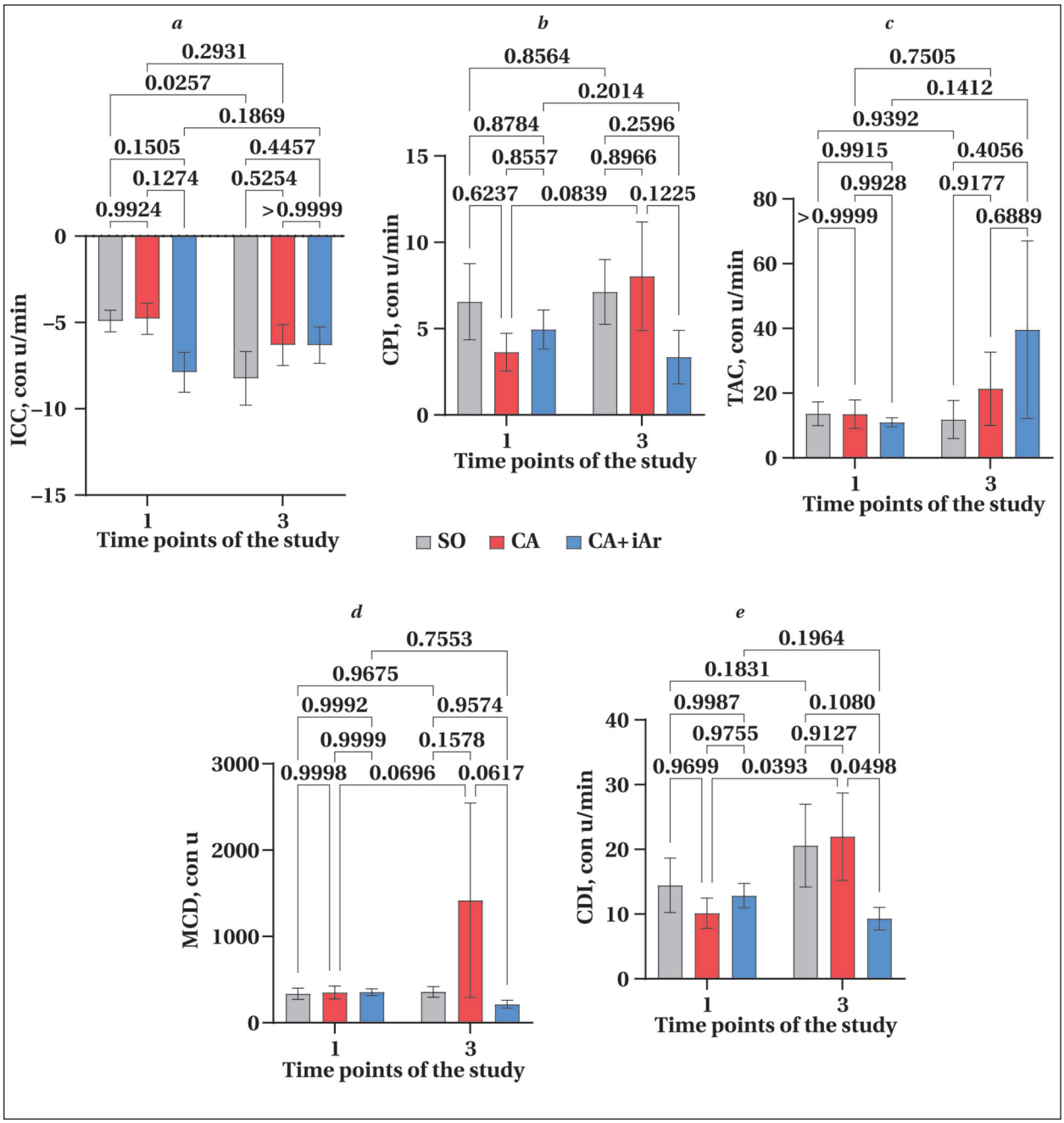

Fig. 6. Coagulation parameters in the study groups.

Thus, the profile observed in the CA+iAr group can be characterized as a selective attenuation of the coagulation response: coagulation is initiated less intensively, clot growth and compaction are slowed down, and the final firmness is lower, while normal retraction and lysis mechanisms are preserved. This pattern of changes can be considered a manifestation of a moderate anticoagulant and antiplatelet effect, directed primarily at the structural and mechanical properties of the forming thrombus.

Such modulation of coagulation can be extremely useful in hypercoagulable status, which often develops in the post-resuscitation period and is associated with the risk of microangiopathy and organ dysfunction [4–6]. However, the number of complications in the CA+iAr group did not differ statistically significantly from other groups. It has previously been shown that inert gases, including argon, can reduce tissue factor expression and platelet activity *in vitro* [19]. Our *in vivo* data confirm this ability of argon under conditions of global ischemic damage.

As for cumulative electrophysiological and molecular data, one can assume that the induction of autophagy (beclin-1 increase) after argon therapy contributes to myocardial cytoprotection, reduces

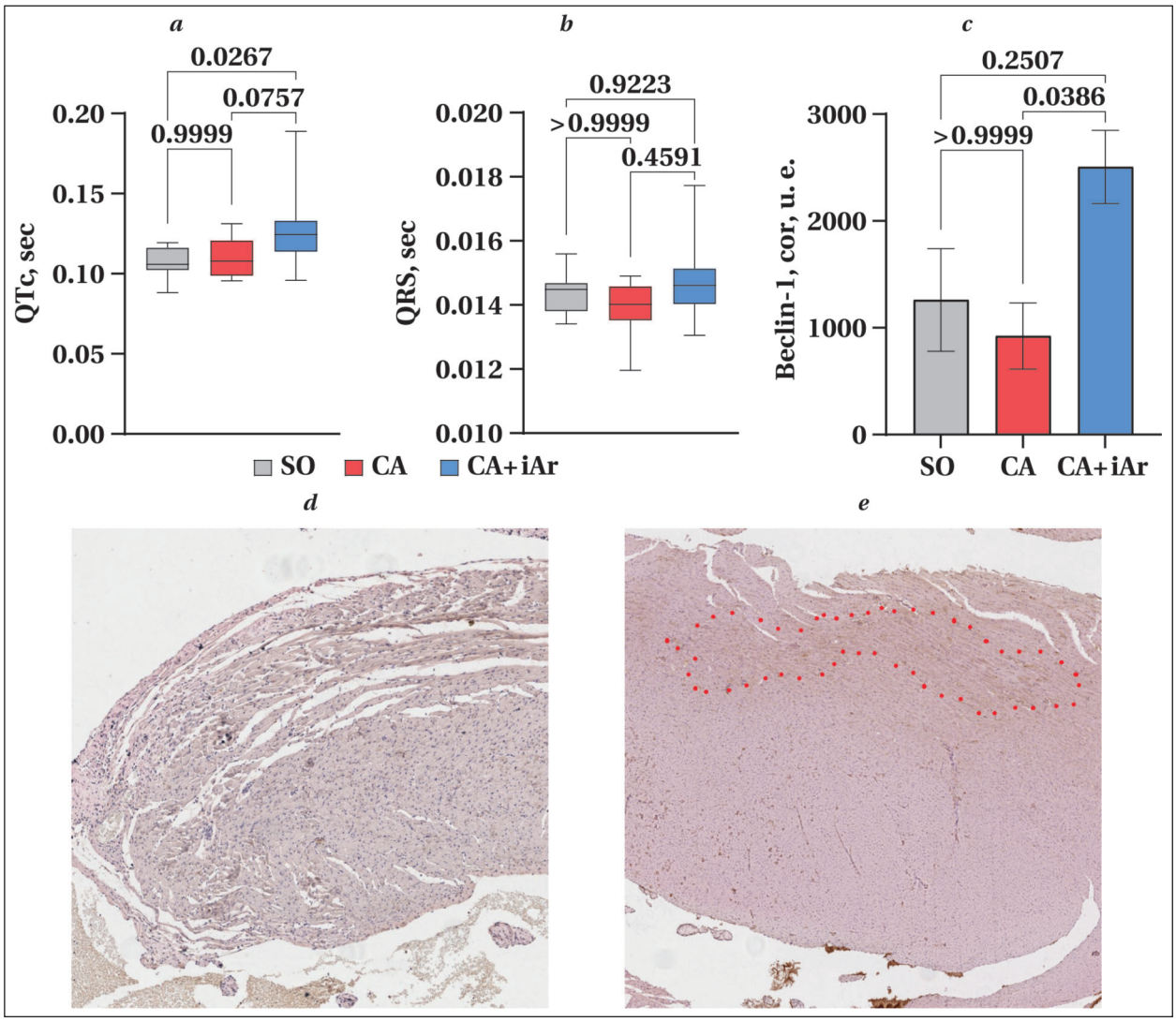

Fig. 7. Electrocardiogram readings at the third time point (*a*, *b*). Number of beclin-1-positive cells in the myocardium (*c*). Images representing myocardial slides in the CA (*d*) and CA+Ar (*e*) groups.
Note. The red dotted line marks the area that is positively stained with beclin-1. * — $p < 0.05$.

damage and variability of myocardial electrical properties, manifested by moderate prolongation of repolarization (QTc) and changes in conductivity (QRS) within normal limits with an intact ST segment. This corresponds to a cardioprotective profile without signs of proarrhythmic risk under the conditions studied, which has been previously described in other models [23, 26].

Analysis of the neurological status of the animals showed marked differences between the groups, indicating the influence of experimental interventions on functional recovery after brain damage.

The data obtained indicate the neuroprotective effect of argon and partial recovery of functional disorders.

Comparing functional data with molecular markers allowed us to hypothesize the basis for this effect of argon. Beclin-1 is a key regulator of autophagy, and its increase in the presence of argon may indirectly reflect the activation of cellular self-regulation and defense mechanisms. Given that autophagy can reduce cellular stress and prevent neuronal apoptosis, the increase in beclin-1 may be one of the factors contributing to the improvement in neurological status of animals in the CA+iAr group.

Thus, the data obtained demonstrate the neuroprotective properties of argon, which has also been shown in other studies [21, 22, 29] and consistent with the concept of argon's multifaceted effect on post-traumatic brain injury: it simultaneously alleviates neurological disorders and activates internal mechanisms of self-regulation and neuron survival.

The decrease in the number of caspase-3+ positive cells in the CA+iAr group compared to the

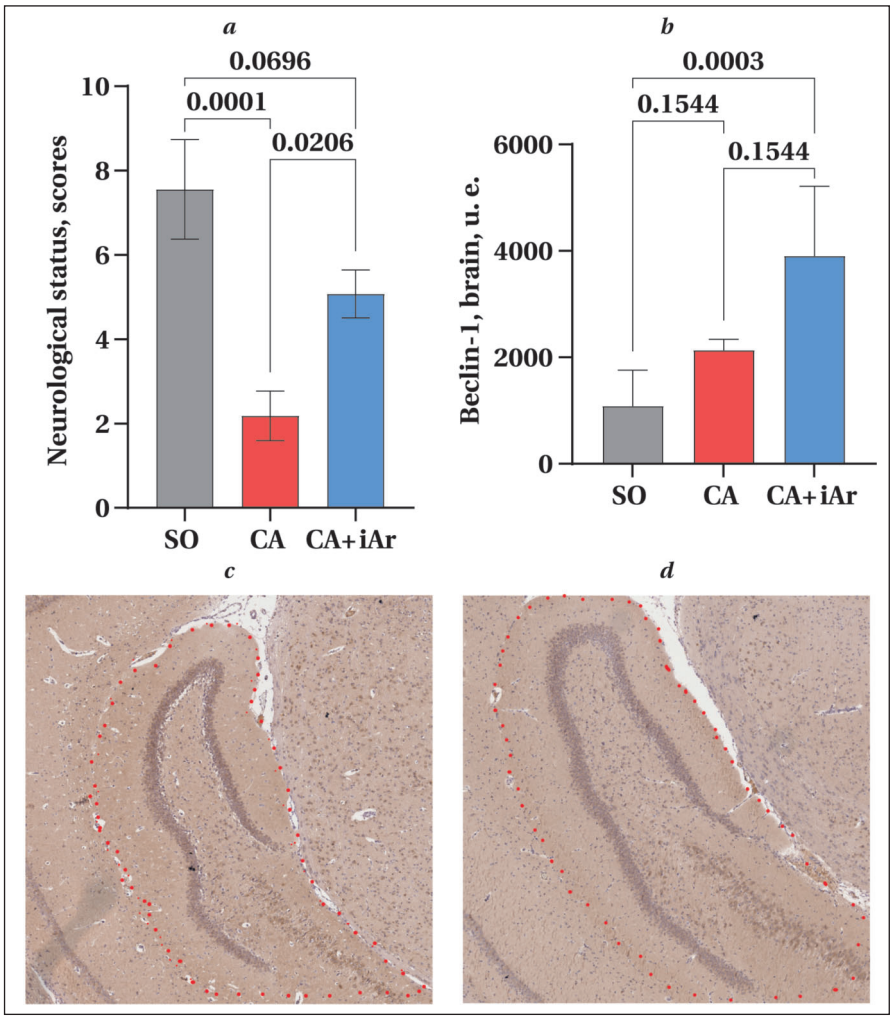

Fig. 8. Neurological assessment parameters at the third time point (*a*). Number of beclin-1 positive cells in the hippocampus (*b*). Images representing hippocampal slides in the CA (*c*) and CA+Ar (*d*) groups.
Note. The red dotted line marks the areas where the count was performed.
* — $p < 0.05$; *** — $p < 0.001$.

CA group indicates the suppression of apoptotic cell death after treatment with argon-oxygen mixture, which is consistent with the known anti-apoptotic properties of argon [14, 16]. Simultaneous decrease of serum neuron-specific enolase (NSE) levels means lower release of this neuronal damage marker, indicating a lower degree of nerve tissue destruction. Taken together, these data suggest that argon inhalation promotes maintenance of cell integrity and reduces the severity of neuronal damage by limiting both apoptosis and necrotic processes, which can be considered a manifestation of its neuroprotective effect.

Limitations and prospects of the study. It should be noted that the study was limited by a short observation window (3 hours after ROSC) and did not allow for the assessment of long-term functional and morphological outcomes. Markers of systemic inflammation and specific molecular pathways (e. g., PI3K/Akt or Nrf2 signaling cascades) that could clarify the targets of argon action were also not investigated. Finally, the choice of dosage and duration of argon therapy was based on preliminary studies and requires further optimization.

Nevertheless, the results of the study suggest that argon may be a promising means of modulating the cellular response to brain injury, providing functional improvement while preserving cellular structure and activating autophagic pathways.

Further research should focus on clarifying the time- and dose-dependent effects of argon use, its molecular targets and mechanisms of action, and in particular the relationship between beclin-1 activation and signaling pathways that provide neuroprotection. It is also necessary to evaluate the long-term outcomes of argon use.

Conclusion

Inhalation of argon-oxygen mixture in the early post-resuscitation period resulted in:

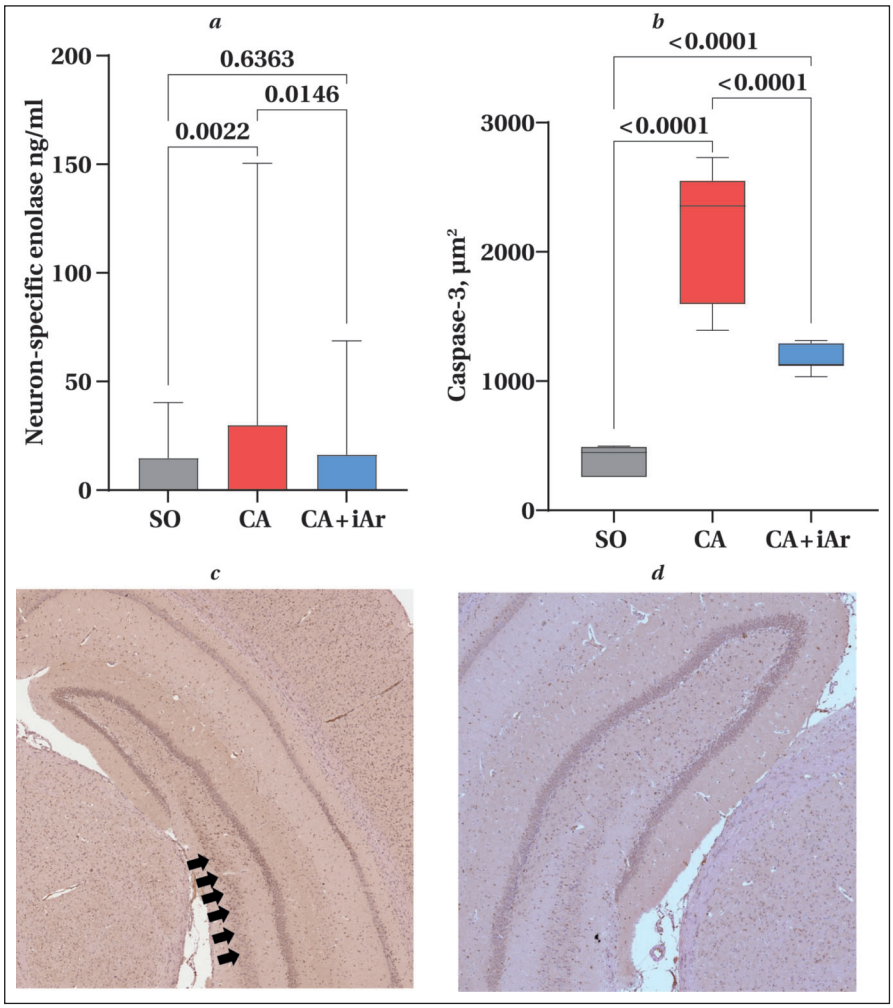

Fig. 9. Neuron-specific enolase (*a*). Number of cas-3 positive cells (*b*). Images representing hippocampal slides in the CA (*c*) and CA+iAr (*d*) groups.
Note. Parameters are presented at the third time point. Black arrows indicate the area of cas-3 positive cells. * — $p < 0.05$; ** — $p < 0.01$; **** — $p < 0.0001$.

— no changes in systemic hemodynamics, cardiac repolarization and conduction;

— decreasing Kv and Sigma values, normalization of blood lactate concentration, pH, and BE parameters;

— an increase in the oxygenation index and beclin-1 content in the lungs, myocardium, and hippocampus;

— a moderate anticoagulant and antiplatelet effect;

— improvement in neurological status parametes;

— reduction in neuron-specific enolase and Cas-3+ cell counts.

Although the differences in physiological parameters between the groups at early time points were minimal, further analysis of microcirculation, coagulation, organ damage biomarkers, and neurological status suggests that argon can effectively modulate key pathophysiological mechanisms of post-resuscitation syndrome.

Our data demonstrate that early inhalation of an argon-oxygen mixture after cardiac arrest provides a multisystem protection by improving oxygenation and microcirculation, promoting the activation of autophagic mechanisms in vital organs, reducing the severity of neuronal damage, and moderately modulating the blood clotting.

In this regard, argon can be considered a promising therapeutic agent for post-resuscitation syndrome.

References

1. *Кузовлев А. Н., Бобошко В. А., Боева Е. А., Григорьев Е. В., Давыдов П. А., Давыдова Л. А., Дежурный Л. И., с соавт.* Остановка сердца (взрослые пациенты). Клинические рекомендации. *Общая реаниматология*. 2025; 21 (4): 5–79. *Kuzovlev A. N., Boboshko V. A., Boeva E. A., Grigoriev E. V., Davydov P. A., Davydova L. A., Dezhurny L. I., et al.* Cardiac arrest in adult patients. Clinical guidelines. *General Reanimatology = Obshchaya Reanimatologiya*. 2025; 21 (4): 5–79. (in Rus.&Eng.). DOI: 10.15360/1813-9779-2025-4-2589.
2. *Barros A. J., Enfield K. B.* In-hospital cardiac arrest. *Emerg Med Clin North Am*. 2023; 41 (3): 455–464. DOI: 10.1016/j.emc.2023.03.003. PMID: 37391244.
3. *Hirsch K. G., Abella B. S., Amorim E., Bader M. K., Barletta J. F, Berg K., Callaway C. W., et al; American Heart Association and Neurocritical Care Society*. Critical care management of patients after cardiac arrest: a scientific statement from the American Heart Association and Neurocritical Care Society. *Circulation*. 2024; 149 (2): e168-e200. DOI: 10.1161/CIR.0000000000001163. PMID: 38014539.
4. *Penketh J., Nolan J. P.* Post-cardiac arrest syndrome. *J Neurosurg Anesthesiol*. 2023; 35 (3): 260–264. DOI: 10.1097/ANA.0000000000000921. : 37192474.
5. *Singh A., Jefferson J.* Post-cardiac arrest care. *Emerg Med Clin North Am*. 2023; 41 (3): 617–632. DOI: 10.1016/j.emc.2023.03.009. PMID: 37391254.
6. *Sandroni C., Cronberg T., Sekhon M.* Brain injury after cardiac arrest: pathophysiology, treatment, and prognosis. *Intensive Care Med*. 2021; 47 (12): 1393–1414. DOI: 10.1007/s00134-021-06548-2. PMID: 34705079.
7. *Sumner B. D., Hahn C. W.* Prognosis of cardiac arrest-peri-arrest and post-arrest considerations. *Emerg Med Clin North Am*. 2023; 41 (3): 601–616. DOI: 10.1016/j.emc.2023.03.008. PMID: 37391253.
8. *Nutma S., Beishuizen A., van den Bergh W. M., Foudraine N. A., le Feber J., Filius P. M.G., Cornet A. D., et al*; GRECO Investigators. Ghrelin for neuroprotection in post-cardiac arrest coma: a randomized clinical trial. *JAMA Neurol*. 2024; 81 (6): 603–610. DOI: 10.1001/jamaneurol.2024.1088. PMID: 38709502.
9. *Nolan J. P., Sandroni C., Böttiger B. W., Cariou A., Cronberg T., Friberg H., Genbrugge C., et al.* European Resuscitation Council and European Society of Intensive Care Medicine guidelines 2021: post-resuscitation care. *Intensive Care Med*. 2021; 47 (4): 369–421. DOI: 10.1007/s00134-021-06368-4. PMID: 33765189.
10. *Yang Y. S., Wu S.H., Chen W. C., Pei M. Q., Liu Y. B., Liu C. Y., Lin S., et al.* Effects of xenon anesthesia on postoperative neurocognitive disorders: a systematic review and meta-analysis. *BMC Anesthesiol*. 2023; 23 (1): 366. DOI: 10.1186/s12871-023-02316-5. PMID: 37946114.
11. *Bezuglov E., Morgans R., Khalikov R., Bertholz V., Emanov A., Talibov O., Astakhov E., et al.* Effect of xenon and argon inhalation on erythropoiesis and steroidogenesis: a systematic review. *Heliyon*. 2023; 9 (5): e15837. DOI: 10.1016/j.heliyon.2023.e15837. PMID: 37215856.
12. *Nair A. S., Christopher A., Pulipaka S. K., Suvvari P., Kodisharapu P. K., Rayani B. K.* Efficacy of xenon anesthesia in preventing postoperative cognitive dysfunction after cardiac and major non-cardiac surgeries in elderly patients: a topical review. *Med Gas Res*. 2021; 11 (3): 110–113. DOI: 10.4103/2045-9912.314330. PMID: 33942781.
13. *Kaufman M. J., Meloni E. G.* Xenon gas as a potential treatment for opioid use disorder, alcohol use disorder, and related disorders. *Med Gas Res*. 2025; 15 (2): 234–253. DOI: 10.4103/mgr.MEDGASRES-D-24-00063. PMID: 39812023.
14. *Balsamo F., Li B., Chusilp S., Lee D., Biouss G., Lee C., Maynes J. T., et al.* Argon inhalation attenuates systemic inflammation and rescues lung architecture during experimental neonatal sepsis. *Pediatr Surg Int*. 2023; 40 (1): 21. DOI: 10.1007/s00383-023-05596-7. PMID: 38108911.
15. *Creed J., Cantillana-Riquelme V., Yan B. H., Ma S., Chu D., Wang H., Turner D. A., et al.* Argon inhalation for 24 h after closed-head injury does not improve recovery, neuroinflammation, or neurologic outcome in mice. *Neurocrit Care*. 2021; 34 (3): 833–843. DOI: 10.1007/s12028-020-01104-0. PMID: 32959200.
16. *Antonova V. V., Silachev D. N., Ryzhkov I. A., Lapin K. N., Kalabushev S. N., Ostrova I. V., Varnakova L. A., et al.* Three-hour argon inhalation has no neuroprotective effect after open traumatic brain injury in rats. *Brain Sci*. 2022; 12 (7): 920. DOI: 10.3390/brainsci12070920. PMID: 35884727.
17. *Silachev D. N., Boeva E. A., Yakupova E. I., Milovanova M. A., Varnakova L. A., Kalabushev S. N., Antonova V. V., et al.* Positive neuroprotective effect of argon inhalation after photochemically induced ischemic stroke model in rats. *Bull Exp Biol Med*. 2023; 176 (2): 143–149. DOI: 10.1007/s10517-024-05984-6. PMID: 38189873.
18. *Antonova V. V., Silachev D. N., Plotnikov E. Y., Pevzner I. B., Ivanov M. E., Boeva E. A., Kalabushev S. N., et al.* Positive effects of argon inhalation after traumatic brain injury in rats. *Int J Mol Sci*. 2024; 25 (23): 12673. DOI: 10.3390/ijms252312673. PMID: 39684384.
19. *Bao L., Liu Y., Jia Q., Chu S., Jiang H., He S.* Argon neuroprotection in ischemic stroke and its underlying mechanism. *Brain Res Bull*. 2024; 212: 110964. DOI: 10.1016/j.brainresbull.2024.110964. PMID: 38670471.
20. *Goebel U., Scheid S., Spassov S., Schallner N., Wollborn J., Buerkle H., Ulbrich F.* Argon reduces microglial activation and inflammatory cytokine expression in retinal ischemia/reperfusion injury. *Neural Regen Res*. 2021; 16 (1): 192–198. DOI: 10.4103/1673-5374.290098. PMID: 32788476.
21. *Motta F., De Giorgio D., Cerrato M., Salmaso A., Magliocca A., Merigo G., Olivari D., et al.* Postresuscitation ventilation with a mixture of argon and hydrogen reduces brain injury after cardiac arrest in a pig model. *J Am Heart Assoc*. 2024; 13 (9): e033367. DOI: 10.1161/JAHA.123.033367. PMID: 38639335.
22. *Fumagalli F, Olivari D., Boccardo A., De Giorgio D., Affatato R., Ceriani S., Bariselli S., et al.* Ventilation with argon improves survival with good neurological recovery after prolonged untreated cardiac arrest in

pigs. *J Am Heart Assoc*. 2020; 9 (24): e016494.
DOI: 10.1161/JAHA.120.016494. PMID: 33289464.
23. *Merigo G., Florio G., Madotto F., Magliocca A., Silvestri I., Fumagalli F., Cerrato M., et al.* Treatment with inhaled argon: a systematic review of pre-clinical and clinical studies with meta-analysis on neuroprotective effect. *EBioMedicine*. 2024; 103: 105143.
DOI: 10.1016/j.ebiom.2024.105143. PMID: 38691938.
24. *Alshami A., Einav S., Skrifvars M. B., Varon J.* Administration of inhaled noble and other gases after cardiopulmonary resuscitation: a systematic review. *Am J Emerg Med*. 2020; 38 (10): 2179–2184.
DOI: 10.1016/j.ajem.2020.06.066. PMID: 33071073.
25. *Magliocca A., Fries M.* Inhaled gases as novel neuroprotective therapies in the postcardiac arrest period. *Curr Opin Crit Care*. 2021; 27 (3): 255–260.
DOI: 10.1097/MCC.0000000000000820.
PMID: 33769417.
26. *Gianni S., Valsecchi C., Berra L.* Therapeutic gases and inhaled anesthetics as adjunctive therapies in critically ill patients. *Semin Respir Crit Care Med*. 2022; 43 (3): 440–452.
DOI: 10.1055/s-0042-1747966. PMID: 35533689.
27. *Дубенский А. Ю., Рыжков И. А., Лапин К. Н., Калабушев С. Н., Варнакова Л. А., Цоколаева З. И., Долгих В. Т., с соавт.* Асфиксическая остановка кровообращения с комплексом реанимационных мероприятий в экспериментальной модели. *Общая реаниматология*. 2024; 20 (2): 55–64. *Dubensky A. Y., Ryzhkov I. A., Lapin K. N., Kalabushev S. N., Varnakova L. A., Tsokolaeva Z. I., Dolgikh V.T et al.* Asphyxial circulatory arrest with a complex of resuscitation measures in an experimental model. *General Reanimatology = Obshchaya Reanimatologiya*. 2024; 20 (2): 55–64. (in Rus.&Eng.).
DOI: 10.15360/1813-9779-2024-2-55-64.
28. *Percie du Sert N., Hurst V., Ahluwalia A., Alam S., Avey M. T., Baker M., Browne W. J., et al.* The ARRIVE guidelines 2.0: Updated guidelines for reporting animal research. *J Cereb Blood Flow Metab*. 2020; 40 (9): 1769–1777.
DOI: 10.1177/0271678X20943823. PMID: 32663096.
29. *Riess M. L., Balzer C., Li Z., Barajas M. B.* Inhaled argon for cardiopulmonary resuscitation: current knowledge and future clinical potential. *Expert Rev Respir Med*. 2025: 1–4.
DOI: 10.1080/17476348.2025.2528944.
PMID: 40590840.

Received 10.09.2025
Accepted 14.01.2026
Online First 09.02.2026